

Phase diagram analysis and crystal growth of solid solutions $\text{Ca}_{1-x}\text{Sr}_x\text{F}_2$

D. Klimm^{a,*}, M. Rabe^a, R. Bertram^a, R. Uecker^a, and L. Parthier^b

^a*Institute for Crystal Growth, Max-Born-Str. 2, 12489 Berlin, Germany*

^b*SCHOTT Lithotec AG, Moritz-von-Rohr-Str. 1a, 07748 Jena, Germany*

Abstract

The binary phase diagram $\text{CaF}_2-\text{SrF}_2$ was investigated by differential thermal analysis (DTA). Both substances exhibit unlimited mutual solubility with an azeotropic point showing a minimum melting temperature of $T_{\min} = 1373^\circ\text{C}$ for the composition $\text{Ca}_{0.582}\text{Sr}_{0.418}\text{F}_2$. Close to this composition, homogeneous single crystals up to 30 mm diameter without remarkable segregation could be grown by the Czochralski method.

Key words: A1 Phase diagrams, A2 Czochralski method, B1 Halides

PACS: 42.25.Lc Birefringence, 81.30.Dz Phase diagrams of other materials, 81.70.Pg Thermal analysis

1. Introduction

The optical properties of calcium fluoride (CaF_2), especially its large transparency range, make this material superior for applications in the short wavelength range, $\lambda < 400 \text{ nm}$. The cubic CaF_2 has an isotropic linear refraction index n but shows for very small λ nonlinear and nonisotropic intrinsic birefringence. Intrinsic birefringence scales with $1/\lambda^2$. At $\lambda = 157 \text{ nm}$ it reaches values up to 11×10^{-7} for CaF_2 , depending on \vec{n} and polarization, which is one order of magnitude more than acceptable for microelectronic lithography. The intrinsic birefringence is of opposite sign in CaF_2 and BaF_2 and mixed crystals $\text{Ca}_{1-x}\text{Ba}_x\text{F}_2$ have been proposed to overcome the problem [2,3]. Optical transparency and lattice constants a_0 of mixed crystals $\text{Ca}_{1-x}\text{Sr}_x\text{F}_2$ and $\text{Sr}_{1-x}\text{Ba}_x\text{F}_2$ were reported by Černevskaja [4,5]. The dependence $a_0(x)$ was found to be almost linear for both systems.

The binary system $\text{CaF}_2-\text{BaF}_2$ was redetermined recently [6] and is quite complicated: The maximal CaF_2 solubility in BaF_2 is $62 \pm 5 \text{ mol\%}$ and the solubility of BaF_2 in CaF_2 is $8 \pm 2 \text{ mol\%}$. As a result of the miscibility gap, fine lamellar structures with lamella thicknesses $\leq 100 \text{ nm}$ can be found in mixed crystals of intermediate composi-

tion and the material must be regarded as non useful for lithography applications.

Some of us reported recently on first promising results with $\text{Ca}_{1-x}\text{Sr}_x\text{F}_2$ mixed crystals [7]. The difference of cationic radii in this system is smaller than in $\text{Ca}_{1-x}\text{Ba}_x\text{F}_2$ (Ca^{2+} : 126 nm, Sr^{2+} : 140 nm, Ba^{2+} : 156 nm) and larger mutual solubility of the fluorides crystallizing in the same (fluorite) structure can be expected. Indeed it could be found in the present work that CaF_2 and SrF_2 exhibit unlimited mutual solubility without miscibility gap.

2. Experimental

A NETZSCH STA 409C thermal analyzer with graphite heater and standard DTA sample holder (thermocouples Pt90Rh10-Pt) was used for DTA measurements with heating/cooling rates of $\pm 10 \text{ K/min}$ in graphite crucibles without lid in an 80 ml/min argon flow of 99.999% purity. Pieces of CaF_2 single crystal (UV optical quality), of crystalline SrF_2 (Merck, 99.99%), or mixtures of them, respectively, with a total mass of 80 – 120 mg were used as samples. In total 10 compositions $\text{Ca}_{1-x}\text{Sr}_x\text{F}_2$ ($0 \leq x \leq 1$) were investigated. Mixing was obtained by a first heating run up to 1510°C and subsequent cooling to 800°C . All DTA curves that are discussed here were obtained in a following second DTA heating run and raw data for the temperature T were stored in the DTA data files.

* corresponding author

Email addresses: klimm@ikz-berlin.de (D. Klimm), lutz.parthier@schott.com (L. Parthier).

Crystal growth was performed in a commercial Czochralski puller (Cyberstar, Grenoble, France) with *rf* heating and automatic diameter control. The experiments were performed with $\text{Ca}_{1-x}\text{Sr}_x\text{F}_2$ batches of 140 – 150 g from graphite crucibles with 120 mm diameter in a gas mixture of 95% Ar (99.999% purity) with 5% CF_4 (99.995% purity).

The chemical composition of $\text{Ca}_{1-x}\text{Sr}_x\text{F}_2$ mixed crystals and of melt remaining in the growth crucibles was measured with an ICP-OES (Inductively Coupled Plasma–Optical Emission Spectroscopy) “IRIS Intrepid HR Duo” (Thermo Elemental, USA). The precision is $\approx 3\%$ relative standard deviation (R.S.D.) for concentrations above background equivalent concentration (BEC).

3. Results

3.1. Thermal analysis and thermodynamic assessment

The 2nd DTA heating curves around the melt peaks of samples $\text{Ca}_{1-x}\text{Sr}_x\text{F}_2$ with 5 (of 11 in total) different molar compositions x are shown in Fig. 1. It should be remarked, that these curves are not yet corrected for T . The calibration of T was performed after the measurements with the melting points of both pure substances $T_f(x = 0) = 1418^\circ\text{C}$ and $T_f(x = 1) = 1477^\circ\text{C}$ [8]. T_f drops from both pure end members (solid lines) to lower values. The minimum melting temperature (taken from the extrapolated onset of the peak) was observed for $x = 0.4651$ (dotted curve in Fig. 1), but the peak onset was only slightly higher (by $\approx 1\text{ K}$) for the neighboring compositions $x = 0.4120$ or $x = 0.5185$, respectively, that are not shown in Fig. 1. Obviously, $T_f(x)$ has a local minimum (azeotropic point) for some composition near $x = 0.4651$.

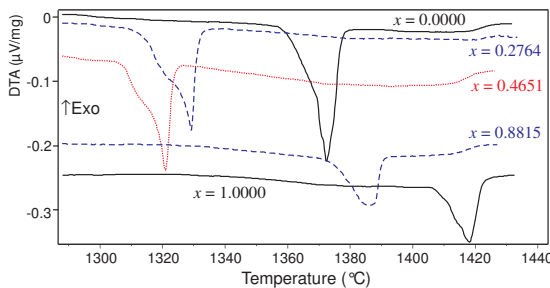


Fig. 1. DTA melting peaks of $\text{Ca}_{1-x}\text{Sr}_x\text{F}_2$ with (from top to bottom) $x = 0.0000$ (pure CaF_2), $x = 0.2764$, $x = 0.4651$, $x = 0.8815$, and $x = 1.0000$ (pure SrF_2). (Raw data, not yet calibrated)

After measurement the contents of the DTA crucible was always molten to a clear sphere. Inspection with an optical microscope did not reveal obvious inclusions.

The experimental points determining the solidus line in the preliminary phase diagram presented on Fig. 2 were taken from the extrapolated onsets (T_{onset}) of the 10 measured compositions after T correction at the T_f of both end members (as written above $T_{\text{sol}} = T_{\text{onset}}$). Unfortunately, the determination of the liquidus from DTA peaks is not

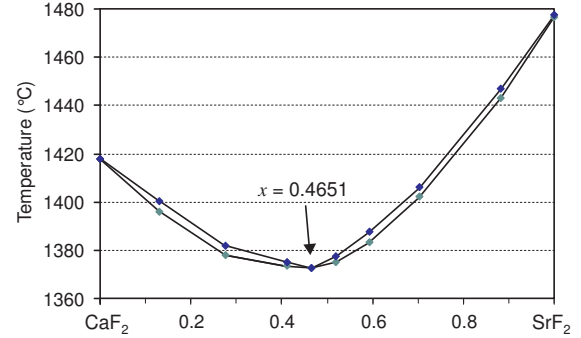


Fig. 2. Binary system $\text{CaF}_2 - \text{SrF}_2$ as obtained from DTA curves (Fig. 1) after T correction.

as straightforward as the determination of the solidus. It turned out that the width of the DTA peaks

$$\Delta T(x) = T_{\text{offset}}(x) - T_{\text{onset}}(x) \quad (1)$$

was 8.1 K for pure CaF_2 ($x = 0.0000$) as well as for $x = 0.4651$, respectively. For pure SrF_2 ($x = 1.0000$) a slightly larger $\Delta T = 9.3\text{ K}$ was found. The experimental points determining the liquidus in Fig. 2 were calculated by

$$T_{\text{liq}}(x) = T_{\text{onset}}(x) + \Delta T(x) - 8.1\text{ K} \\ = T_{\text{offset}}(x) - 8.1\text{ K} \quad (2)$$

with a maximum measured $\Delta T = 12.3\text{ K}$ that was observed for $x' = 0.5932$ and for $x'' = 0.1317$. Procedure (2) results in a difference of 1.2 K between the solidus and liquidus for pure SrF_2 which is regarded as the experimental error.

The thermodynamic assessment was started with the data for the pure end members, CaF_2 and SrF_2 , from the ChemSage database SPS96TO2 [8]. Three mixed phases were calculated, each with species CaF_2 and SrF_2 and for the whole composition range $0 \leq x \leq 1$:

gas: IDMX model (ideal mixing)

liquid: SUBI (two-sublattice ionic solution)

(Ca,Sr)F₂(ss): SUBL (ideal sublattice solution)

Both non-ideal models of mixing take into account that anions and cations are mixing independently. The Gibbs free energy of both non-ideal mixed phases (G_{mixed}) with interacting Ca^{2+} and Sr^{2+} occupying the cation lattice in presence of F^- on the anion lattice can then be described as the sum of the summands G_0 (weighed contribution of the pure components), G_{id} (contribution of an ideal mixture), and G_{ex} (contribution of non-ideal interaction):

$$G_{\text{mixed}} = G_0 + G_{\text{id}} + G_{\text{ex}} \quad (3)$$

$$G_0 = (1 - x)G^{\text{Ca}} + xG^{\text{Sr}} \quad (4)$$

$$G_{\text{id}} = RT ((1 - x)\ln(1 - x) + x\ln x) \quad (5)$$

$$G_{\text{ex}} = (1 - x)x(a_1 + b_1T + d_1T^2 + a_3(2x - 1)) \quad (6)$$

(All data are given here in J/mol or in K.) G^{Ca} or G^{Sr} , respectively, are the database standard values for the pure fluorides [8]. Four parameters for the solid phase and two parameters for the liquid phase were found sufficient for a

satisfactory fit of the experimental data using the ChemSage parameter optimization module. These data are $a_1 = 2046.1957$, $b_1 = -2.3570417$, $d_1 = -0.0045433252$, $a_3 = -844.93984$ for the mixed crystal $(\text{Ca},\text{Sr})\text{F}_2\langle\text{ss}\rangle$ and $a_1 = -43.004897$ and $b_1 = -11.559429$ for the liquid phase. The deviation from ideality is much smaller for the liquid as compared to the solid.

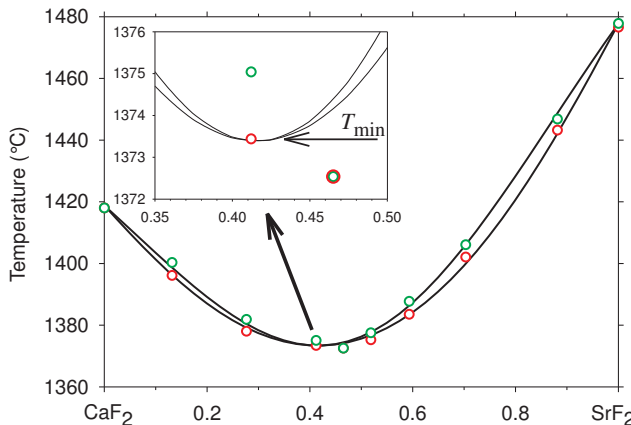


Fig. 3. Thermodynamic assessment of the CaF_2 – SrF_2 phase diagram (lines) together with the experimental points for liquidus and solidus from Fig. 2.

Fig. 3 compares the result of the assessment (3)–(6) with the experimental points. The remaining difference is smaller 1 K — indicating that the thermodynamic models for the G_{ex} are reasonable. Note that the azeotropic point of the assessment $x(T_{\min}) \approx 0.418$ does not coincide with the lowest experimental point that was found at $x = 0.4651$ (insert in Fig. 3).

3.2. Crystal Growth and Characterization

For the crystal growth experiments powdered CaF_2 and SrF_2 from GFI “crystal grade” was used. The SrF_2 concentration was $0.38 \leq x \leq 0.479$ and the pulling rate 1.5 – 2 mm/h for crystals with 18 mm diameter. Some crystals were grown with larger diameter up to 30 mm (Fig. 4).



Fig. 4. CaF_2 – SrF_2 mixed crystal grown at the composition $\text{Ca}_{0.585}\text{Sr}_{0.415}\text{F}_2$ with 30 mm diameter and 50 mm length of the cylinder.

The concentrations of calcium ($1 - x$) and strontium (x) were measured by ICP-OES at the shoulder and bottom, respectively, of several 18 mm crystals and in the remaining melt. It must be expected that only for growth runs without segregation x is constant for all 3 measurements, and

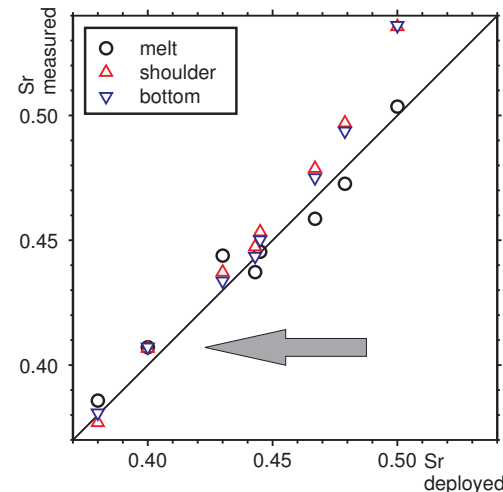


Fig. 5. Strontium concentration (expressed as molar fraction x of SrF_2) in the starting composition (x_0) compared to measured concentrations in the shoulder and bottom of Czochralski crystals and the remainder of the melt (x_{meas}). The straight line is $x_{\text{meas}} = x_0$.

moreover that x equals the Sr concentration in the starting material. Fig. 5 compares the Sr concentration in the starting material (“Sr deployed” = x_0) with the measured x_{meas} . It can be seen that only for $x = 0.40$ the Sr concentration is the same for the 2 positions in the crystal and for the melt. The small positive deviation from the ideality line $x_{\text{meas}} = x_0$ is attributed to experimental errors of the concentration measurement.

4. Summary

It could be confirmed by DTA that CaF_2 and SrF_2 show complete miscibility in both liquid and solid phases. Mixed crystals $\text{Ca}_{1-x}\text{Sr}_x\text{F}_2$ were grown in the concentration range $0.38 \leq x \leq 0.479$ by the Czochralski method. Both DTA and crystal growth experiments showed that the liquidus and solidus lines of the binary phase diagrams meet at a common minimum (azeotropic point) $x \gtrsim 0.4$ with $T_{\min} = 1373^\circ\text{C}$. A Thermodynamic assessment of the DTA melting curves showed the azeotropic point at $x(T_{\min}) \approx 0.418$. Homogeneous $\text{Ca}_{0.582}\text{Sr}_{0.418}\text{F}_2$ single crystals can be grown at this point from the melt as no segregation must be expected.

References

- [1] Y. I. Sirotin, M. P. Shaskolskaya, Fundamentals of Crystal Physics, Mir Publishers, Moscow, 1982.
- [2] J. H. Burnett, Z. H. Levine, E. L. Shirley, Hidden in plain sight: Calcium fluoride’s intrinsic birefringence, *Photonics Spectra* (2001) 88–92.
- [3] J. H. Burnett, Z. H. Levine, E. L. Shirley, Intrinsic birefringence in calcium fluoride and barium fluoride, *Phys. Rev. B* 64 (2002) 241102.

- [4] E. G. Čhernevskaya, Mixed single crystals CaF_2 – SrF_2 and SrF_2 – BaF_2 and their response on γ -radiation, *Optika i Spektroskopija* 10 (1961) 640–643, *in Russian*.
- [5] E. G. Čhernevskaya, G. V. Ananeva, On the structure of mixed crystals between CaF_2 , SrF_2 , BaF_2 , *Fizika Tverdogo Tela* 8 (1966) 216–219, *in Russian*.
- [6] P. P. Fedorov, I. I. Buchinskaya, N. A. Ivanovskaya, V. V. Konovalova, S. V. Lavrishchev, B. P. Sobolev, CaF_2 – BaF_2 phase diagram, *Doklady Physical Chemistry* 401 (2005) 652–654.
- [7] L. Parthier, G. Wehrhan, C. Pötsch, G. V. der Gönna, D. Klimm, R. Uecker, Growth and properties of homogenous mixed crystals $\text{Ca}_{1-x}\text{Sr}_x\text{F}$ for DUV applications, in: Third Asian Conference on Crystal Growth and Crystal Technology, Beijing, Oct. 16–19, 2005.
- [8] GTT Technologies, Kaiserstr. 100, 52134 Herzogenrath, Germany, ChemSage 4.20, <http://www.gtt-technologies.de/> (2000).